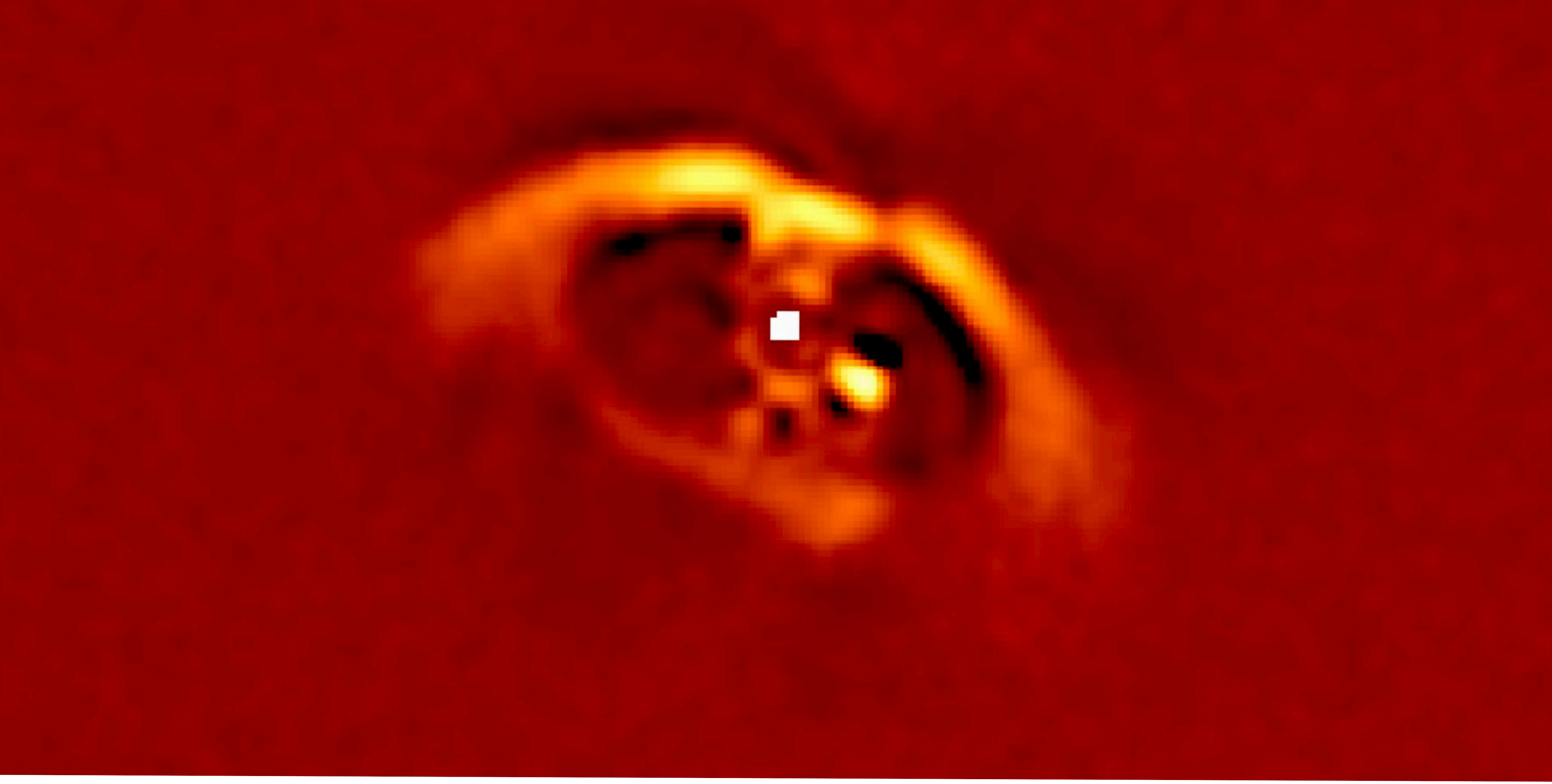

Applying new data analysis methods to SPHERE data to recover debris disks intensity and polarimetry

M. Langlois and DDISK project team

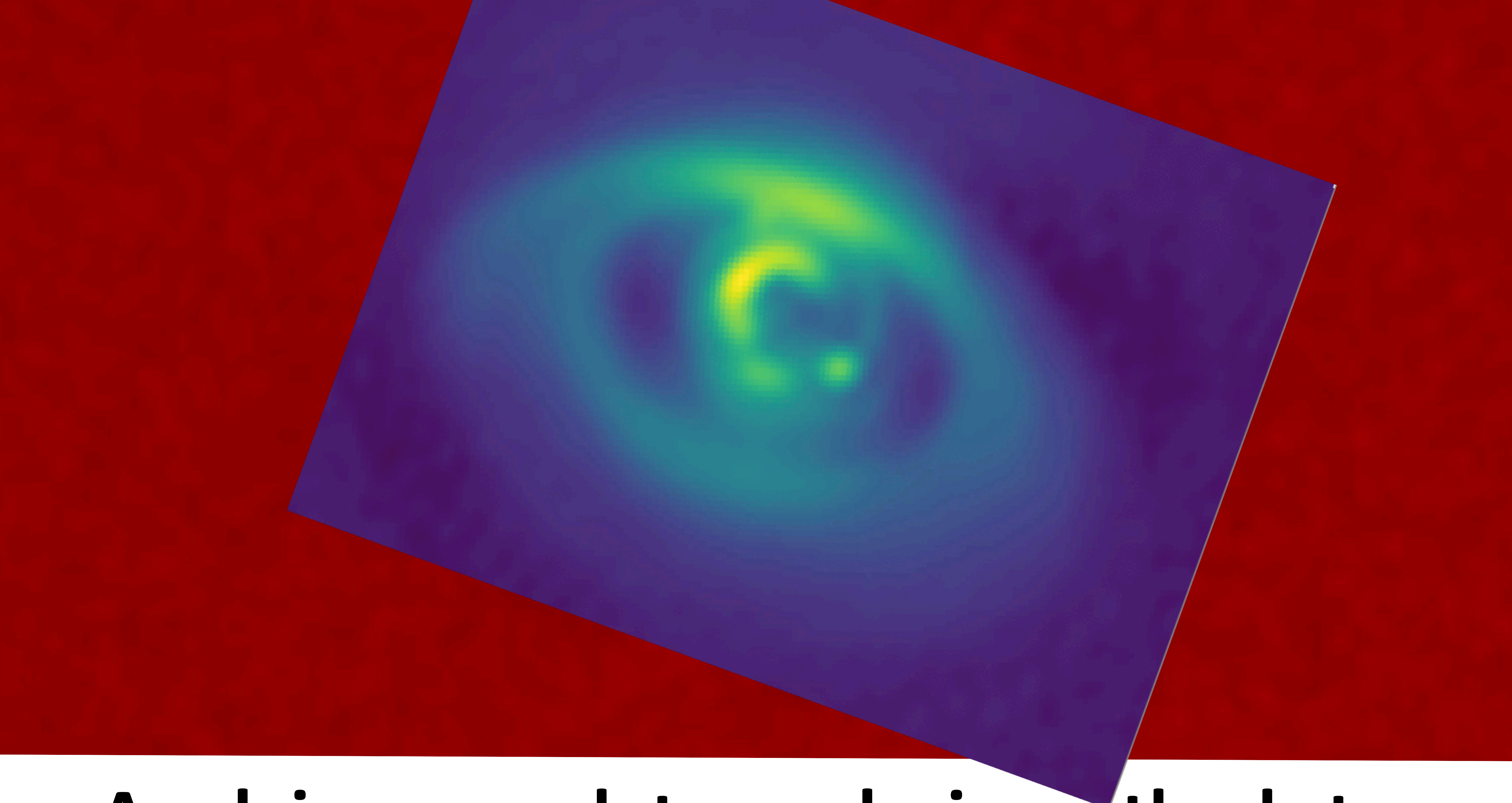

Applying new data analysis methods to SPHERE data to recover debris disks intensity and polarimetry

M. Langlois and DDISK project team

High Contrast Imaging Context

Large HCI Vis_NIR multi-mode datasets
-Imaging
-Polarimetry
-Spectroscopy (LSS+IFS)

Data Analysis Algorithms
-REXPACO
-RHAPSODIE
-PIC
-Deconvolution
-Inverse problems
-Machine learning

Data analysis facility
-Data mining
-Homogeneous analysis
-Survey

Gain
-Sensibility
-Angular resolution
-Robustness
-Accuracy

Observables
-Total intensity distribution
-Polarized intensity distribution
-Spectral Reflectance distribution
-Phase function (color)
-Linear degree of Polarisation (color)

Interpretation
-Disk shape
-Composition
-dust size/Porosity
-Disk-Exoplanets interactions
-Exoplanet formation
-Statistical Analysis/new detections

Disk Numerical Modeling
-Synthetic database
-Hydrodynamic, radiative transf
-Dust/agregate model

Total Intensity – REXPACO Principle I

Forward model

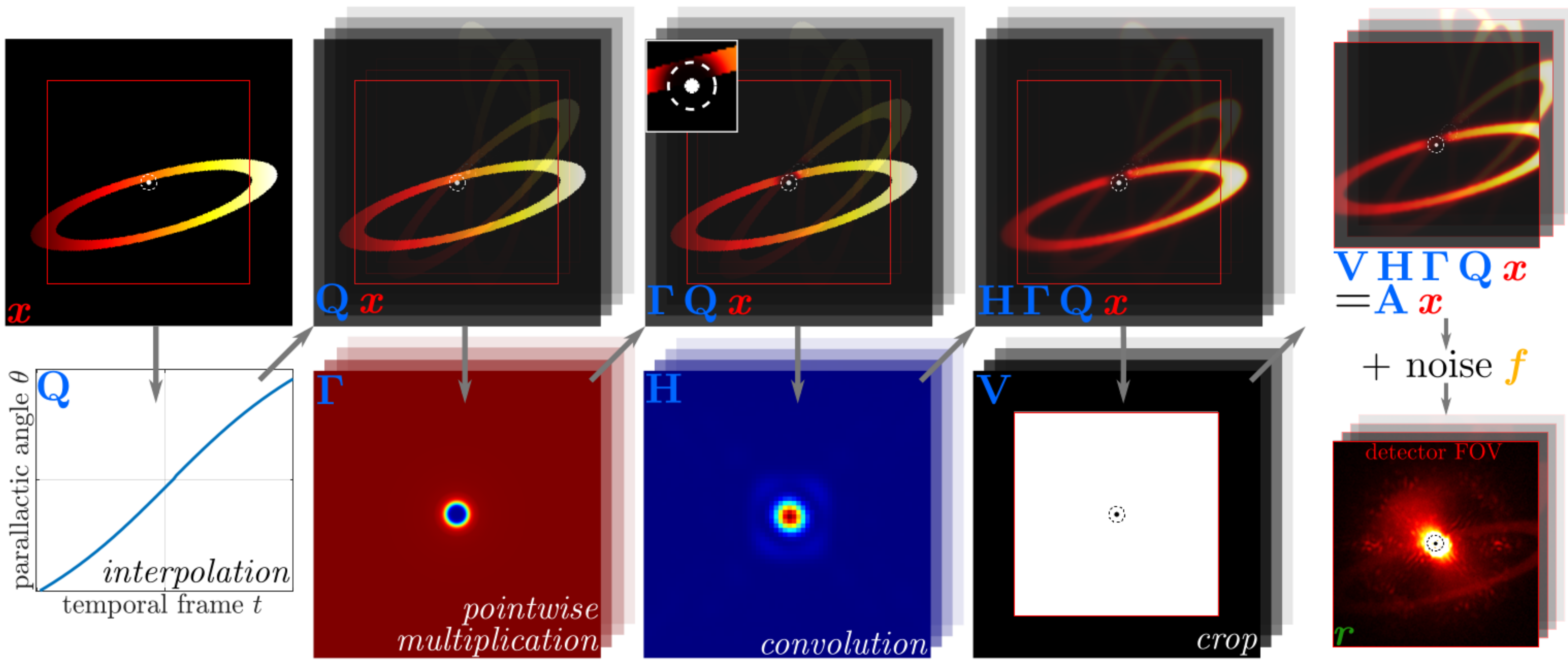

O. Flasseur et al., Astronomy & Astrophysics, vol. 651, A62, *2021*

Total Intensity – REXPACO Principle II

Background fluctuations

Statistical background model

Gaussian Scale Mixture (GSM) to model a **patch**

patch $\boldsymbol{f}_{n,t}$ at pixel n and time t: $\boldsymbol{f}_{n,t} = \boldsymbol{m}_n + \boxed{\sigma_{n,t}}\boldsymbol{u}_{n,t}$ where $\boldsymbol{u}_{n,t} \sim \mathcal{N}(\mathbf{0}, \mathbf{C}_n)$

$$\mathsf{p}_f(\{\boldsymbol{f}_{n,t}\}_{t=1:T}) = \prod_{t=1}^{T} \mathcal{N}\left(\boldsymbol{f}_{n,t} \,\middle|\, \boldsymbol{m}_n, \boxed{\{\sigma_{n,t'}\}_{t'=1:T}}, \mathbf{C}_n\right) \quad \text{where} \quad n = \lfloor \phi_t \rceil$$

Statistical learning

Estimated through **fixed-point iterations**:

- Scaling factor: $\boxed{\widehat{\sigma}^2_{n,t}} = (1/K)\,(\boldsymbol{r}_{n,t} - \boldsymbol{m}_{n,t})\mathbf{C}_n^{-1}(\boldsymbol{r}_{n,t} - \boldsymbol{m}_{n,t})^{\mathrm{t}}$.
- Sample mean: $\widehat{\boldsymbol{m}}_n = \left(\sum_{t=1}^{T} \boxed{\dfrac{1}{\sigma^2_{n,t}}}\boldsymbol{r}_{n,t}\right) \Big/ \left(\sum_{t=1}^{T} \boxed{\dfrac{1}{\sigma^2_{n,t}}}\right)$.
- Sample cov.: $\widehat{\mathbf{S}}_n = \frac{1}{T}\sum_{t=1}^{T} \boxed{\dfrac{1}{\sigma^2_{n,t}}}(\boldsymbol{r}_{n,t} - \boldsymbol{m}_{n,t})(\boldsymbol{r}_{n,t} - \boldsymbol{m}_{n,t})^{\mathrm{t}}$.
- *Shrunk* cov. [Ledoit&Wolf, 2004]; [Chen *et al.*, 2010]: $\widehat{\mathbf{C}}_n = (1 - \widehat{\rho}_n)\widehat{\mathbf{S}}_n + \widehat{\rho}_n\widehat{\mathbf{F}}_n$.

Total Intensity – REXPACO Principle III

Regularized reconstruction framework

Model of the observed intensity

$$\boldsymbol{r} = \mathbf{A}\,\boldsymbol{x} + \boldsymbol{f}\,,$$

- $\boldsymbol{r}$ $(\mathbb{R}^{N\times T})$: total intensity in ADI stack of T frames with N pixels,
- $\boldsymbol{x}$ $\left((\mathbb{R}^{+})^{M}\right)$: unknown object flux,
- $\mathbf{A}$ $(\mathbb{R}^{M} \to \mathbb{R}^{N\times T})$: linear operator describing the image formation,
- $\boldsymbol{f}$ $(\mathbb{R}^{N\times T})$: background; $\boldsymbol{f} \gg \mathbf{A}\,\boldsymbol{x}$, nonstat. w.r.t space & time.

Regularized reconstruction of the object flux

Resolution of an inverse problem:

$$\widehat{\boldsymbol{x}} = \underset{\boldsymbol{x}>\mathbf{0}}{\arg\min}\{\mathscr{C}(\boldsymbol{r},\boldsymbol{x},\mathbf{A},\boldsymbol{\Omega},\boldsymbol{\mu}) = \mathscr{D}(\boldsymbol{r},\mathbf{A}\,\boldsymbol{x},\boldsymbol{\Omega}) + \mathscr{R}(\boldsymbol{x},\boldsymbol{\mu})\}\,,$$

- $\mathscr{D}(\boldsymbol{r},\mathbf{A}\,\boldsymbol{x},\boldsymbol{\Omega})$: data-fidelity term, depends on $\boldsymbol{\Omega}$ statistics of $\boldsymbol{f}$,
- $\mathscr{R}(\boldsymbol{x},\boldsymbol{\mu})$: regularization term, depends on hyperparameters $\boldsymbol{\mu}$.

$\Rightarrow$ $\boldsymbol{f}(\boldsymbol{\Omega})$: local modeling of nonstationary spatial correlations

Performances on Synthetic Disks (IRDIS)

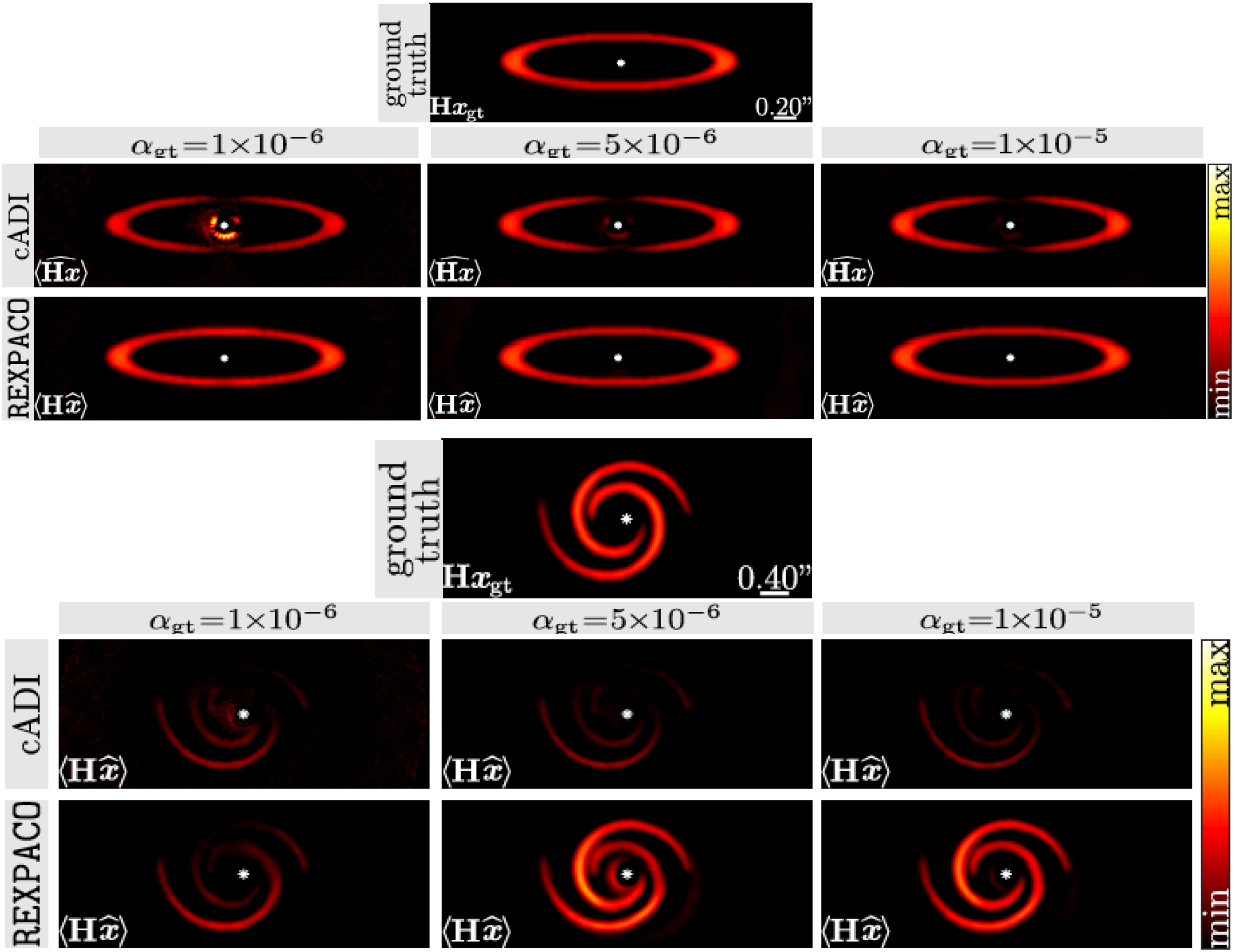

Real Disks Total Intensity (IRDIS)

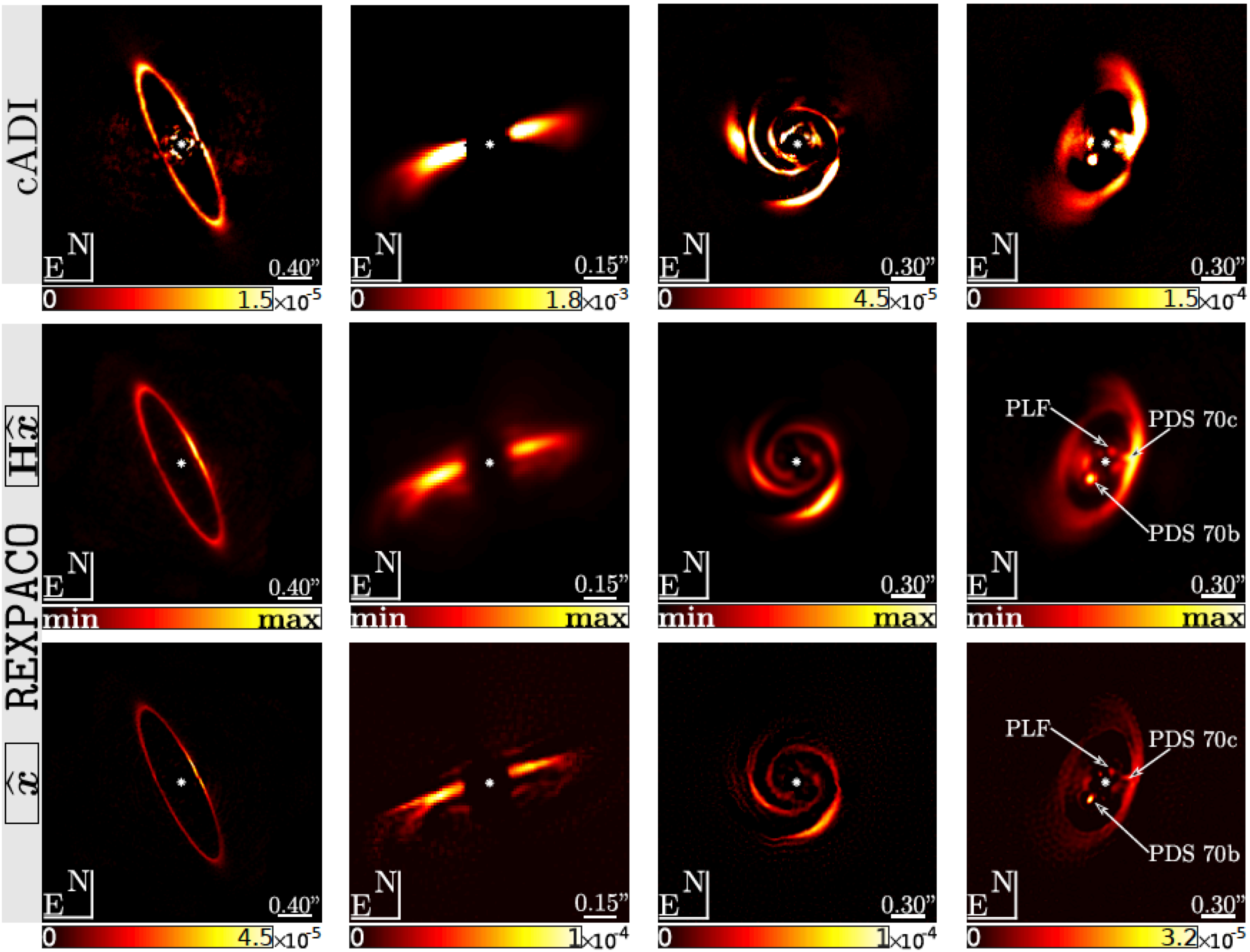

Total Intensity – Multi-Spectral Gain

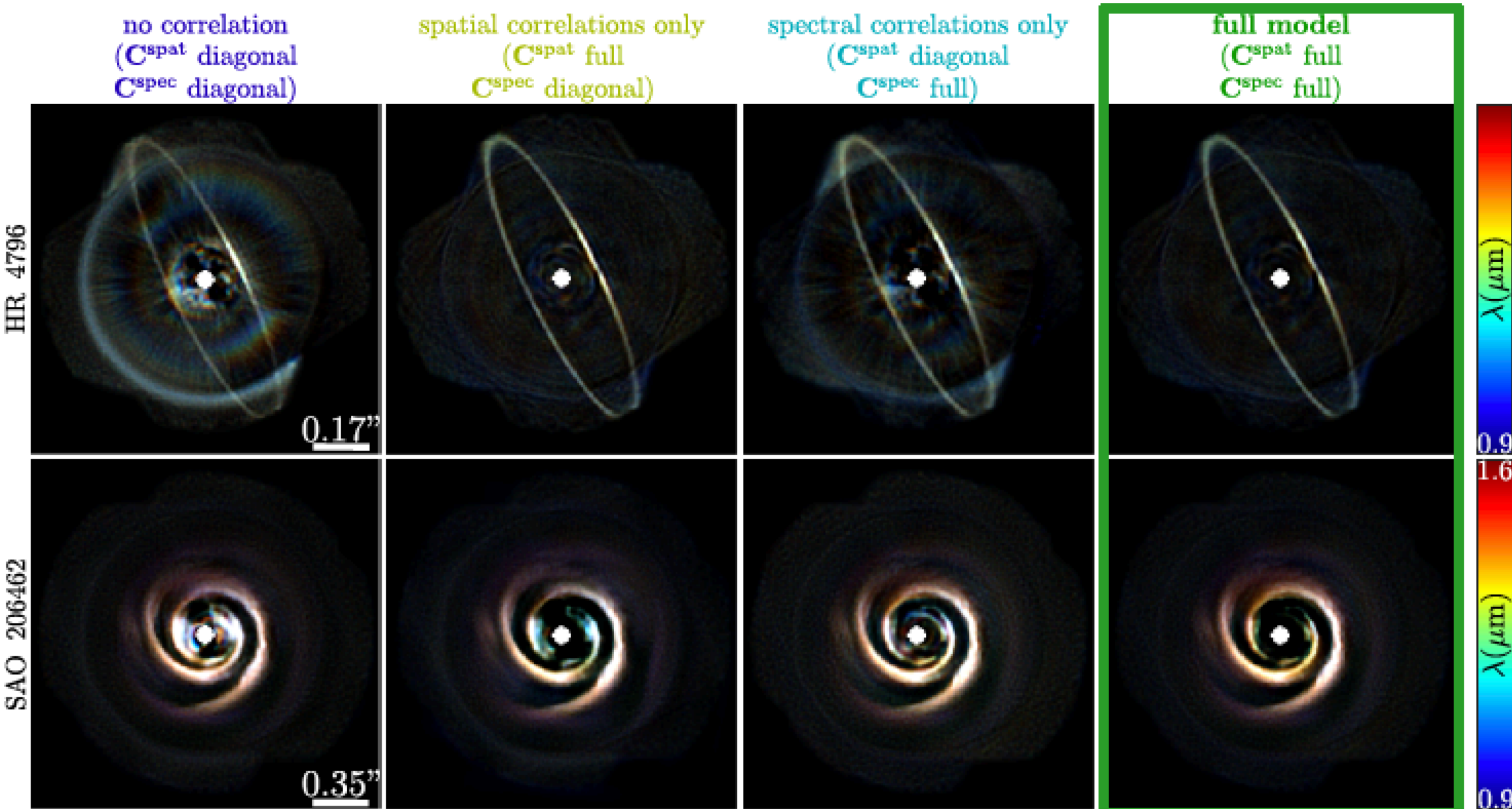

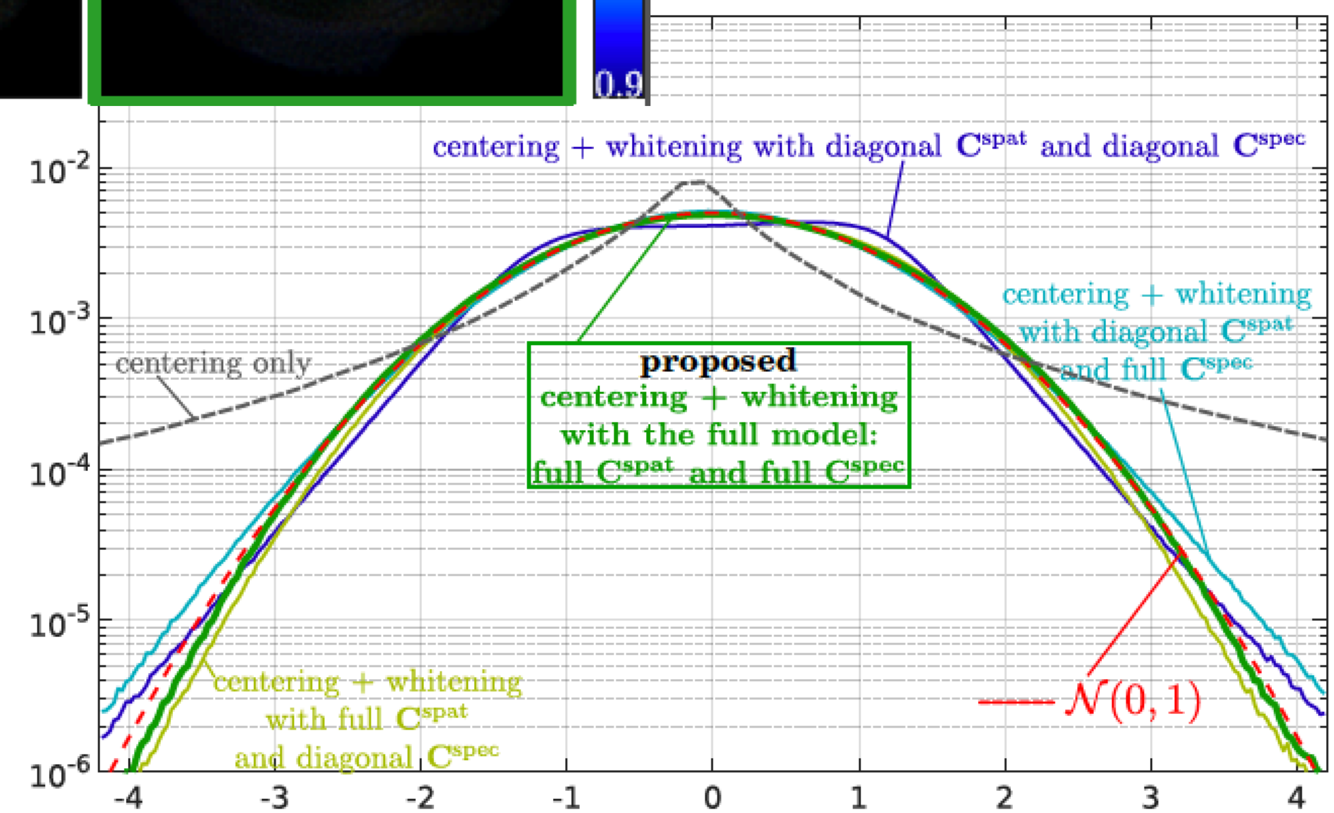

Important benefits from the spectral diversity to recover symetrical disk features whith REXPACO thanks to the spatial temporal covariances modelisation

Real Disks Total Intensity (IFS)

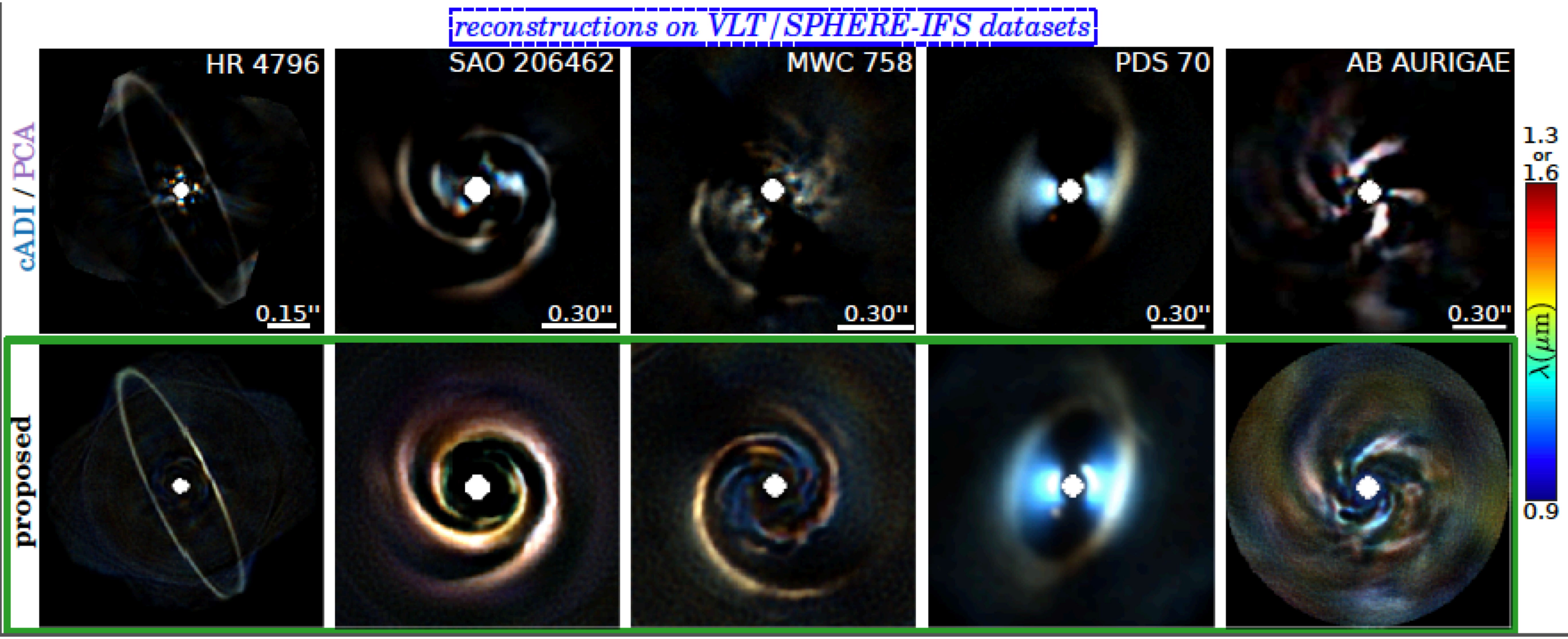

Important benefits from the spectral diversity to recover symetrical disk feature

O. Flasseur, S. Thé, L. Denis, E. Thiébaut, M. Langlois submitted

Polarimetry & deconvolution - RHAPSODIE

From the physics of the instrument to the physical model

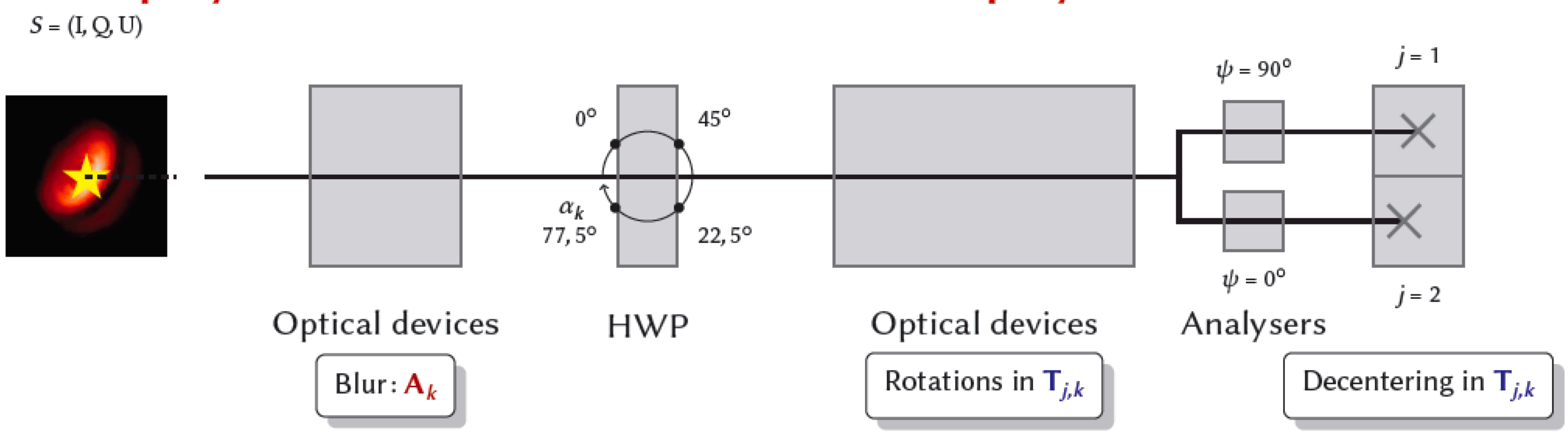

$$S_j^{\mathrm{det}} = \underbrace{\mathbf{M}_j^{\mathrm{pol}}\,\mathbf{T}(-\theta^{\mathrm{der}})\,\mathbf{M}^{\mathrm{der}}\,\mathbf{T}(\theta^{\mathrm{der}})\,\mathbf{T}(-\alpha_k)\,\mathbf{M}^{\mathrm{HWP}}\,\mathbf{T}(\alpha_k)\,\mathbf{M}^{\mathrm{M4}}\,\mathbf{T}(\theta^{\mathrm{alt}})\,\mathbf{M}^{\mathrm{UT}}\,\mathbf{T}(\theta^{\mathrm{par}})}_{\begin{pmatrix} \nu_{j,k,1} & \nu_{j,k,2} & \nu_{j,k,3} \\ \cdot & \cdot & \cdot \\ \cdot & \cdot & \cdot \end{pmatrix}} S$$

$$\mathrm{I}_{j,k}^{\mathrm{det}} = \mathbf{T}_{j,k}\mathbf{A}_k\left[\nu_{j,k,1}\,\mathrm{I} + \nu_{j,k,2}\,\mathrm{Q} + \nu_{j,k,3}\,\mathrm{U}\right].$$

$k \in \{1, \dots K\}$ is the number an observation in a dataset.

L. Denneulin, M. Langlois, N. Pustelnik, E. Thiébaut, A&A 653 June 2021

Polarimetry & deconvolution - RHAPSODIE

Comparison to the state-of-the-art on simulated data

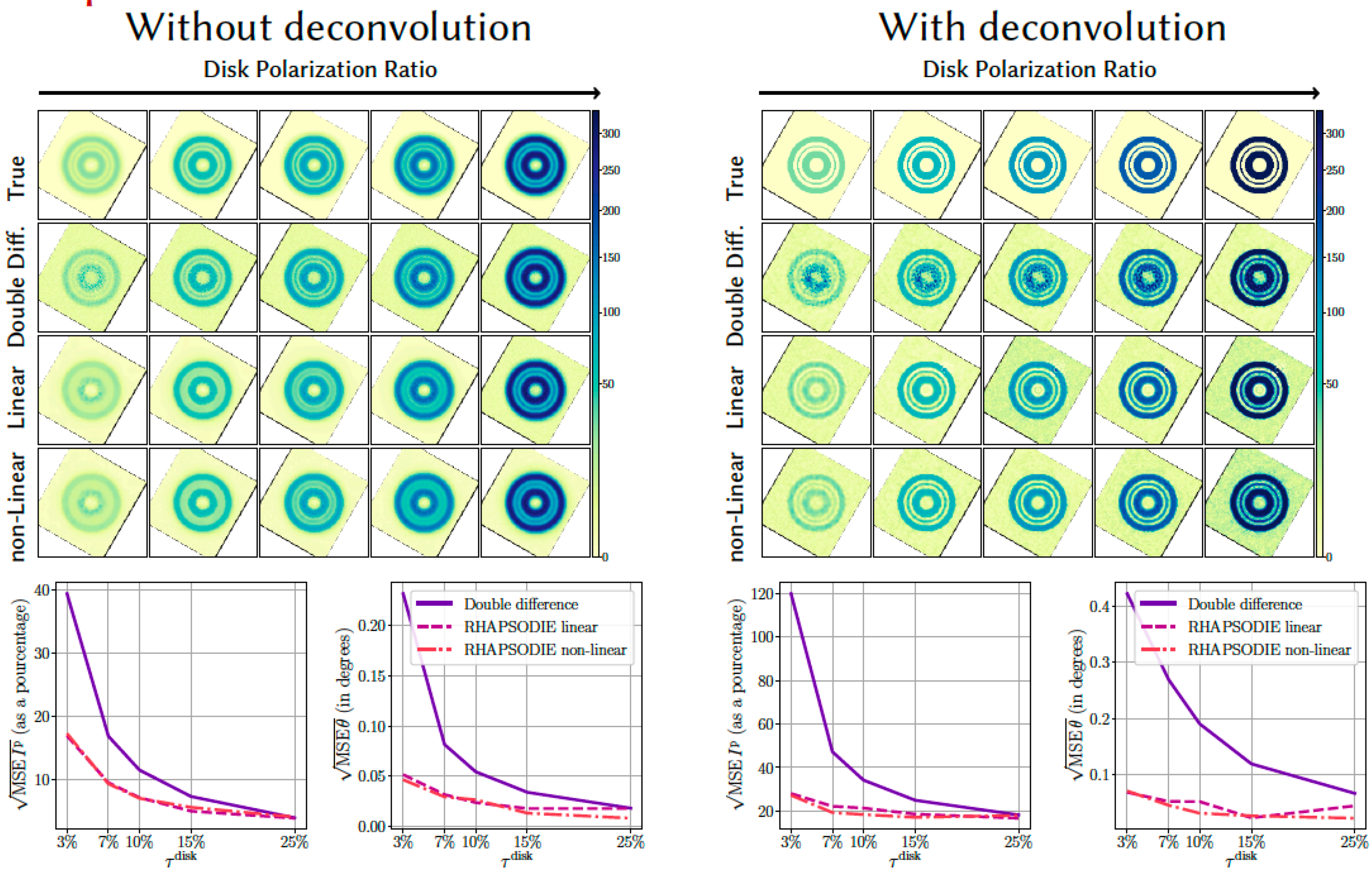

L. Denneulin, M. Langlois, N. Pustelnik, E. Thiébaut, A&A 653 June 2021

Real Disks Polarized Intensity (IRDIS)

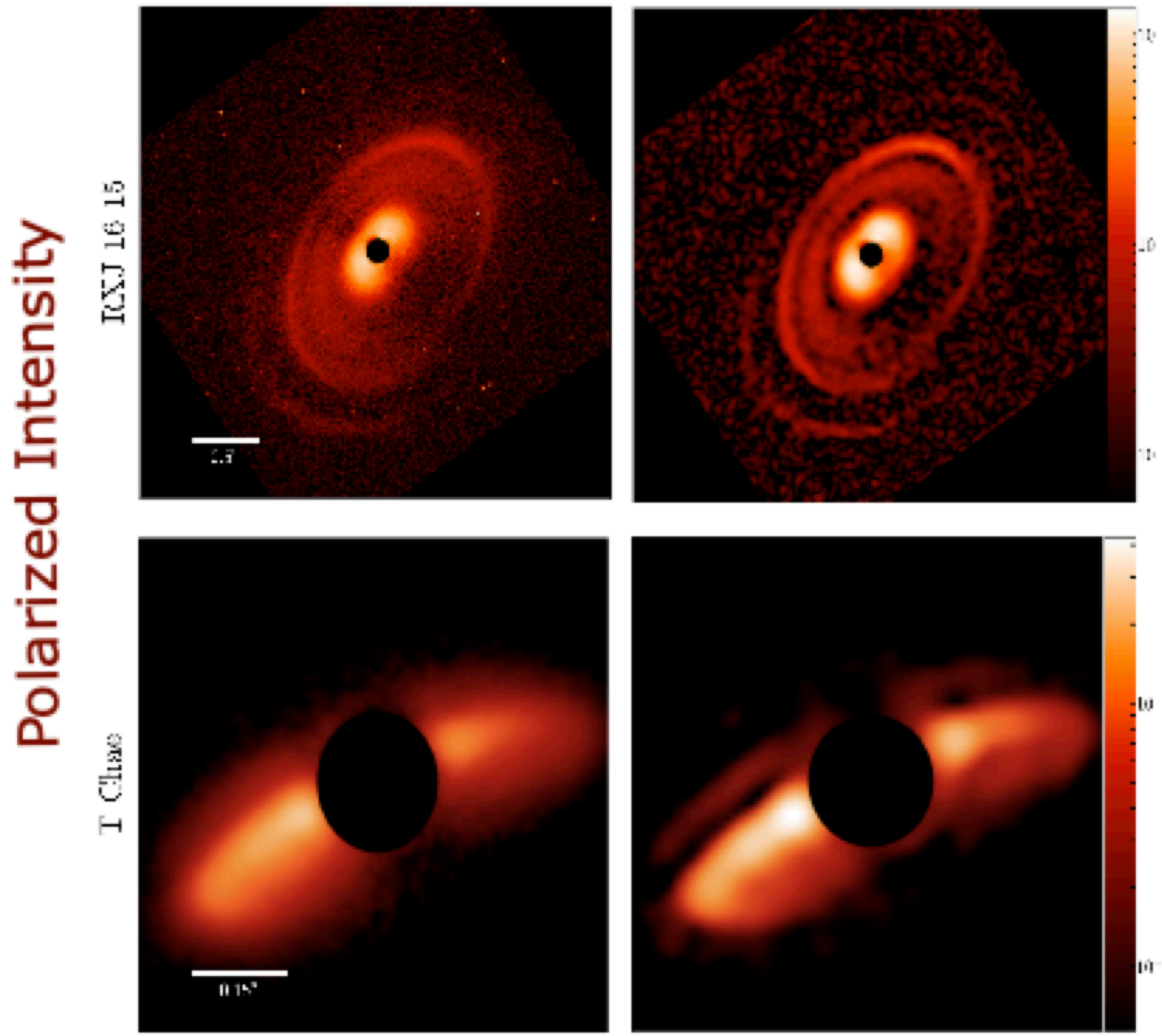

Polarized intensity obtained for IRDIS DPI from the state of the art (Left) and reduced with RHAPSODIE including deconvolution (Right).
Deconvolution improves the angular resolution and thus access to finer disks structures.

Real Disks Polarized Intensity (IRDIS)

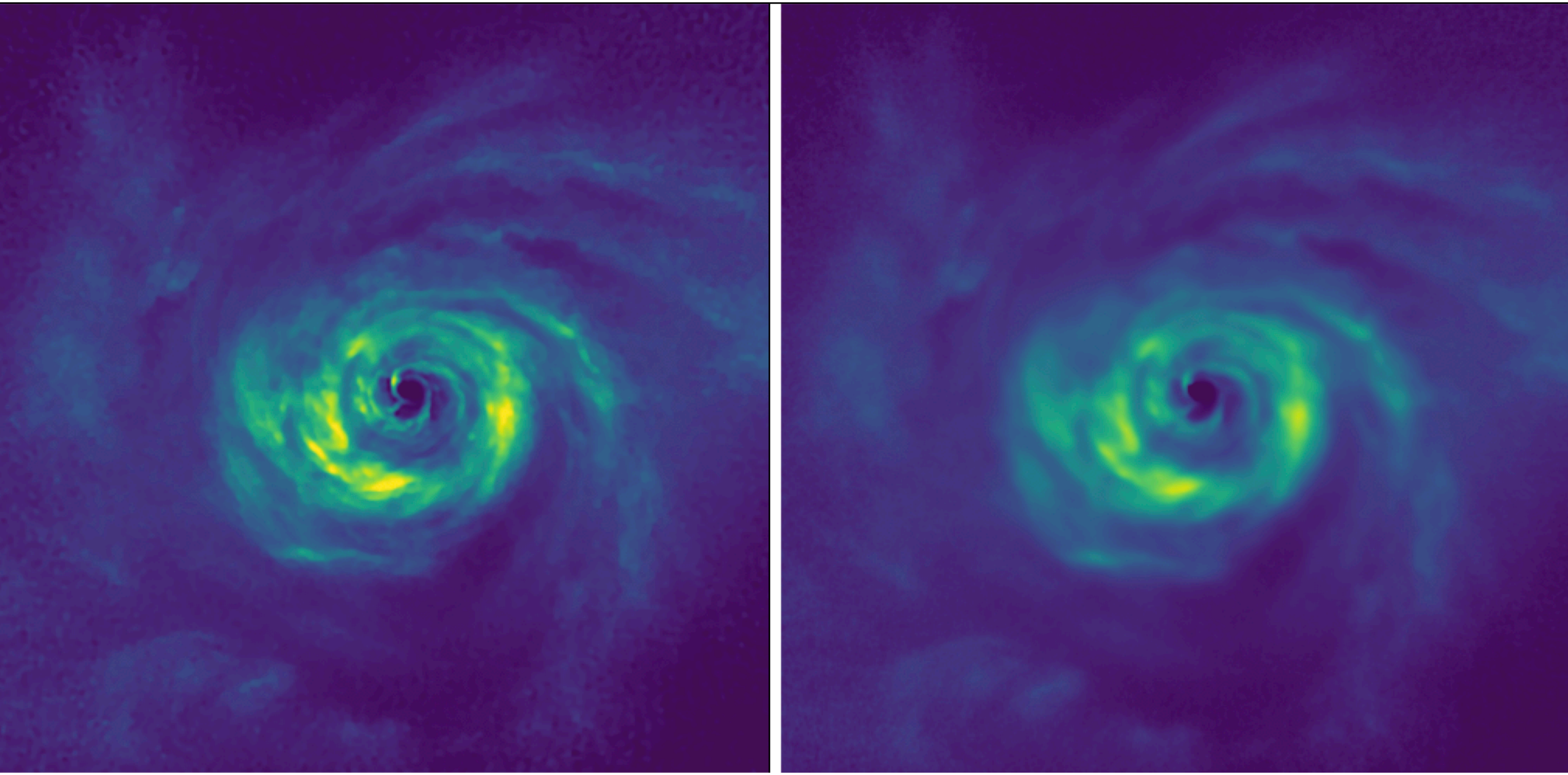

SPHERE showing the formation site of a giant planet in the gas rich young disk AB Aurigae (2.4 $M_\odot$, 1-5 Myr, 163 pc, V = 7; H = 5).

Combining Polarized Total Intensity – AB Aur

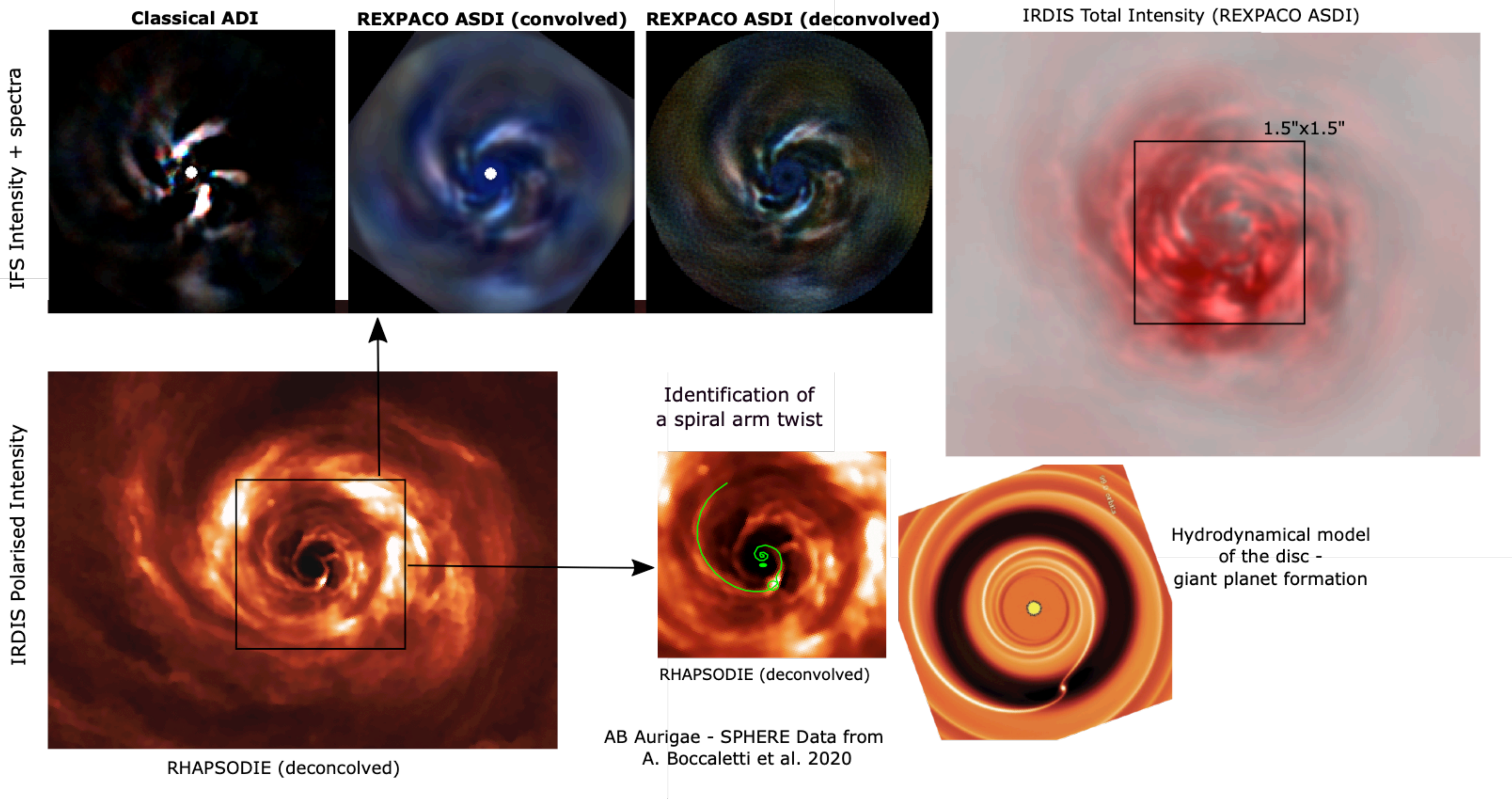

SPHERE (IFS and IRDIS) showing the formation site of a giant planet in the gas rich young disk AB Aurigae (2.4 $M_{\odot}$, 1-5 Myr, 163 pc, V = 7; H = 5). The Top-Right images show the total intensity obtained from the IFS and reduced with REXPACO. The lower part of the image shows the Polarized intensity obtained from IRDIS DPI and reduced with RHAPSODIE (deconvolved).

DPI with deconvolution - RHAPSODIE

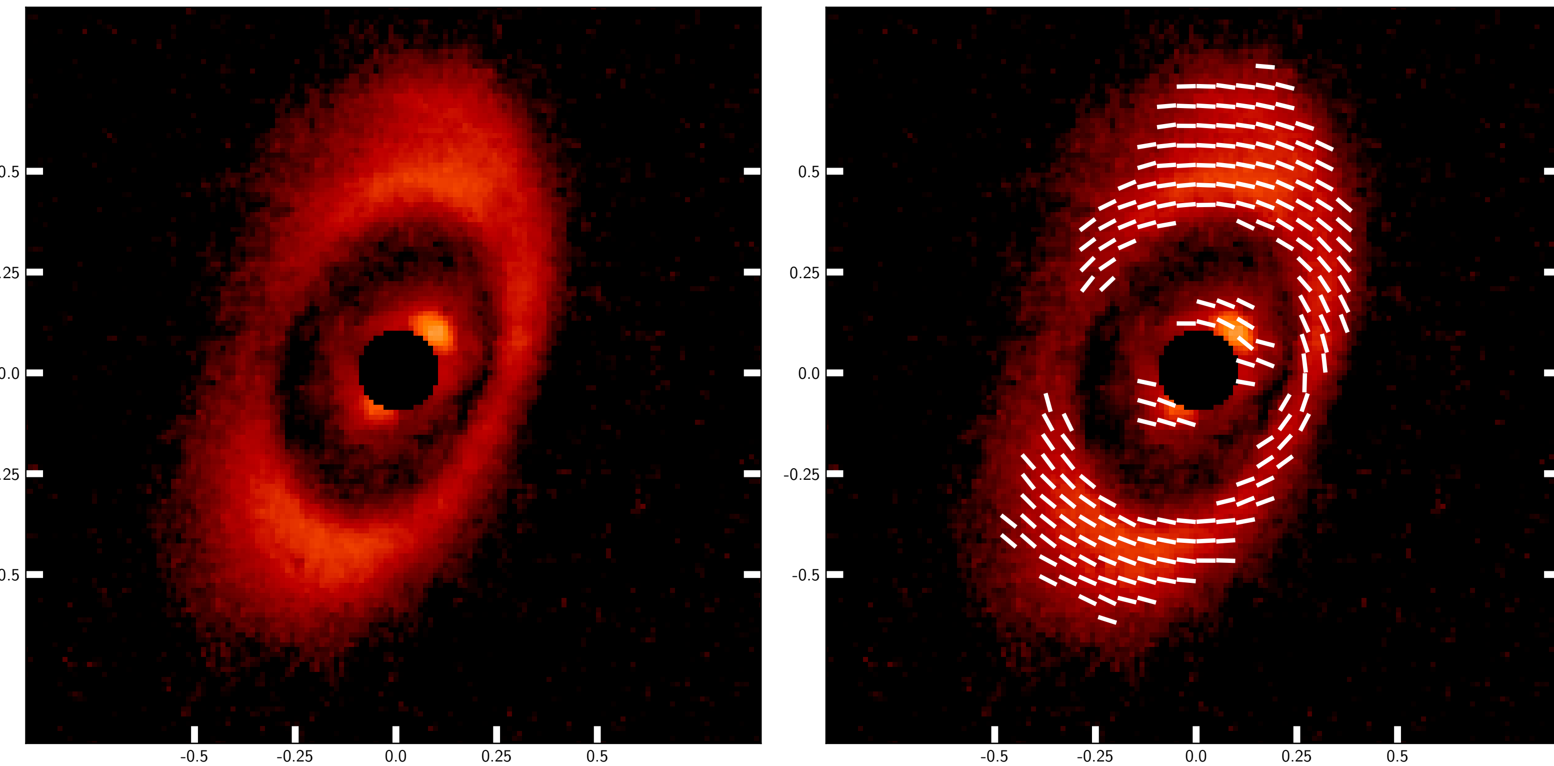

Ip - No deconvolution

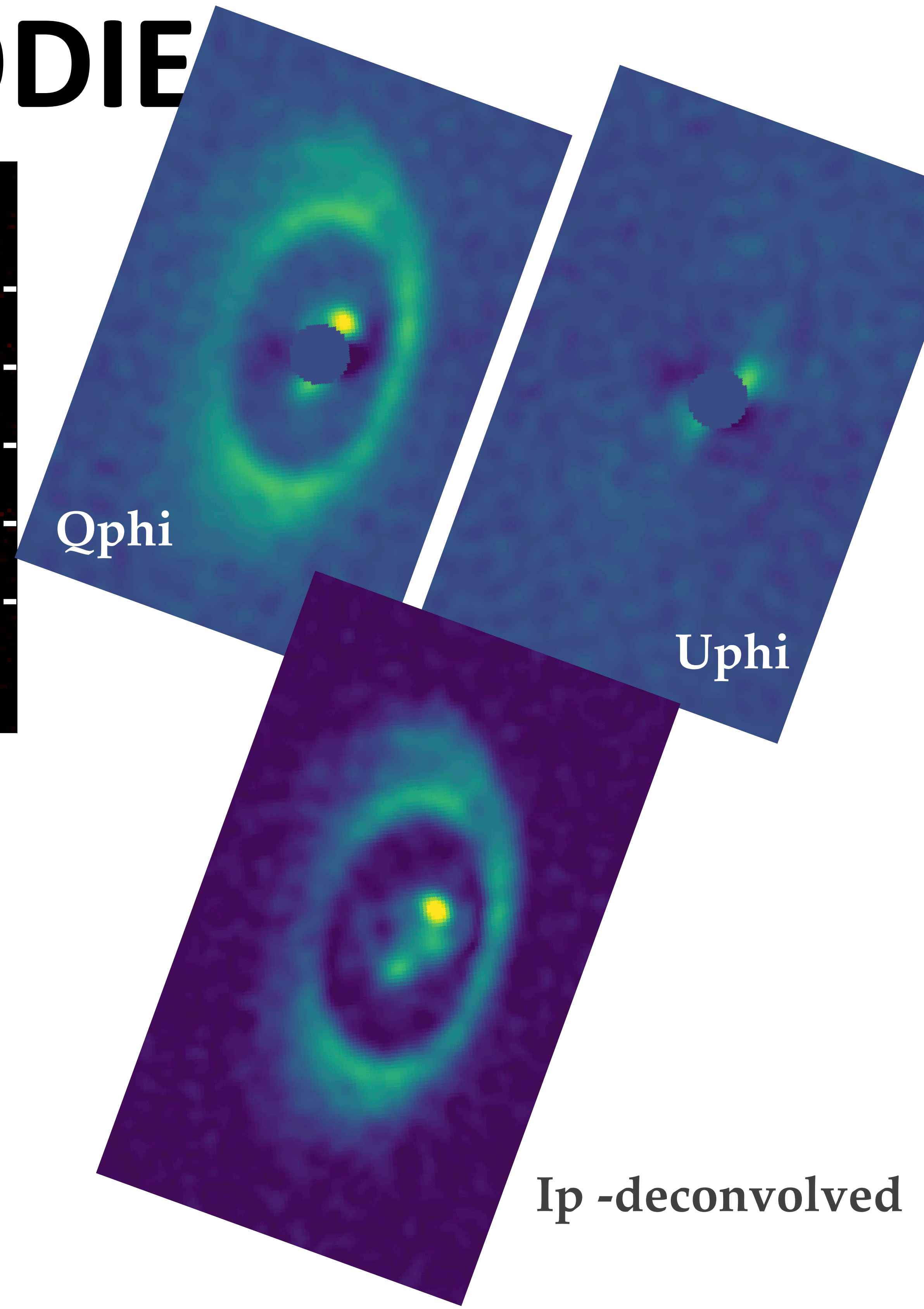

Ip -deconvolved

- Dataset 2019 (IRDIS Ks- ADI+DPI)
- IRDAP instrumental polarisation applied (no compensation of the stellar polarisation)

L. Denneulin, M. Langlois, N. Pustelnik, E. Thiébaut, A&A under revision

Combining Polarized Total Intensity - PDS 70

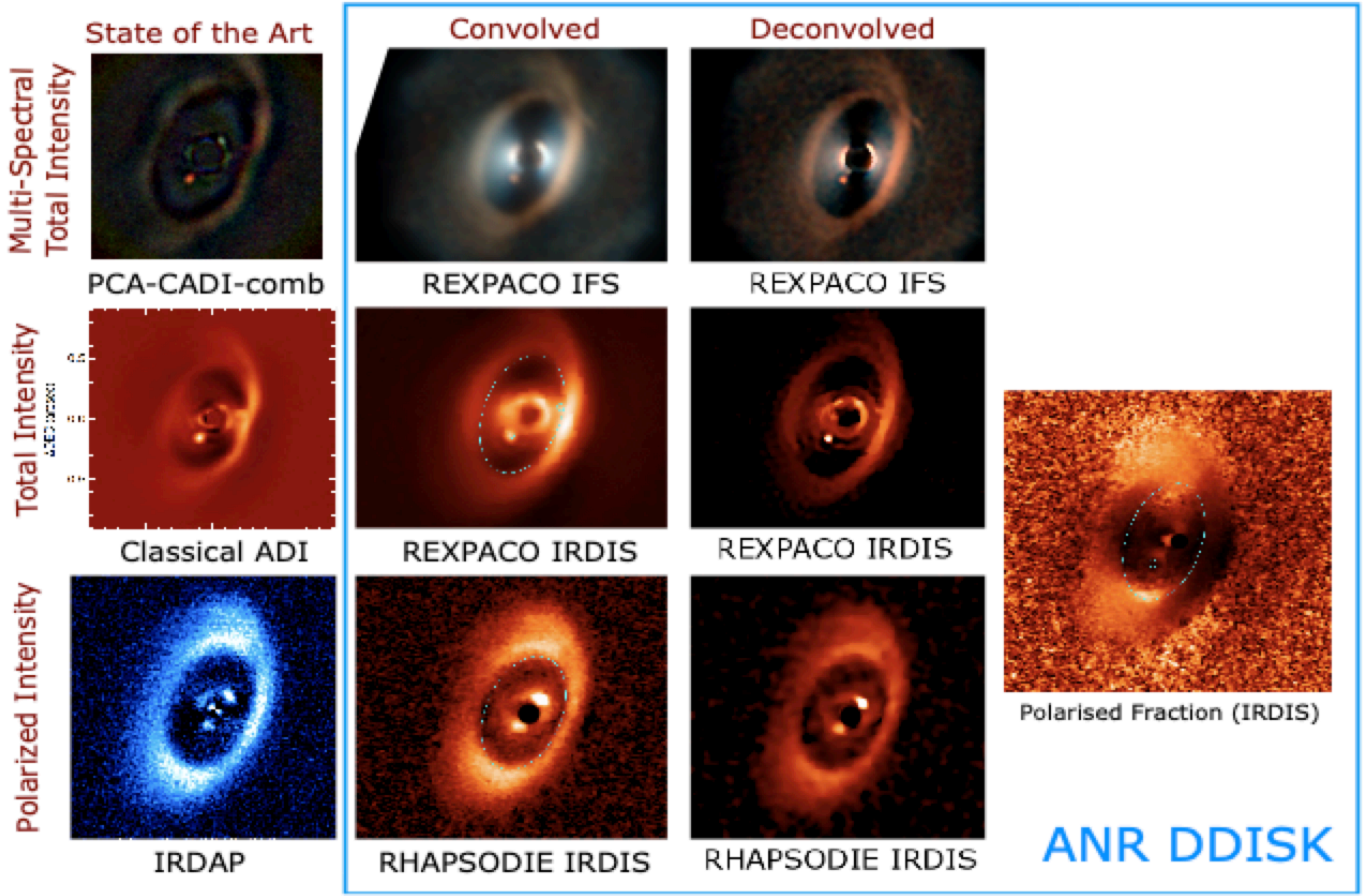

Summary & Futur Plans

Toward a better understanding of the physical processes taking place

- Benefits from new data reduction methods (REXPACO, RHAPSODIE)

- Combining deconvolved polarized intensity and multispectral total intensity (simultaneous ADI+DPI sequence can be analysed in //)

- Finer & deeper morphological studies of the disks (wraps, shadow features, inner part including fainter features)

- Dust properties: Multi wavelength analysis (fluffy vs. Compact, brightness profile, color + polarimetry, polarized fraction & phase function)

- Constraining disk-planet interactions

Thanks